Please cite this articla as, "Tafsirojjaman T, Fawzia S, Thambiratnam D, Zhao XL. Behaviour of CFRP strengthened CHS members under monotonic and cyclic loading. Compos Struct 2019;220:592–601."

# Behaviour of CFRP Strengthened CHS Members under Monotonic and Cyclic Loading

T. Tafsirojjaman [a], Sabrina Fawzia [a,*], David Thambiratnam [a], Xiao-Ling Zhao [b]

[a] School of Civil Engineering and Built Environment, Faculty of Science and Engineering, Queensland University of Technology, 2 George Street, Brisbane, QLD 4000, Australia.

[b] Department of Civil and Environmental Engineering, The University of New South Wales (UNSW), Sydney, NSW 2052, Australia

([*]Corresponding Author: sabrina.fawzia@qut.edu.au, Tel: 61731381012, Fax: 61 7 31381170

Email addresses: tafsirojjaman@hdr.qut.edu.au(T. Tafsirojjaman), sabrina.fawzia@qut.edu.au (S. Fawzia), d.thambiratnam@qut.edu.au (D. Thambiratnam), zxl@monash.edu (X. L. Zhao)

## ABSTRACT

Tubular hollow members, though used in many civil and mechanical applications, are highly vulnerable structural elements when subjected to cyclic loading. They have been used extensively in both onshore and offshore civil infrastructure where cyclic loading can result from earthquake, waves, currents and wind. Thus, tubular hollow steel members may be required to undergo strengthening to withstand both static and cyclic loads. In the present study externally-bonded carbon fibre reinforced polymer (CFRP) has been used to strengthen the circular hollow section (CHS) steel specimens. A series of experiments on bare and CFRP strengthened CHS steel specimens subjected to monotonic and cyclic loading at the tip has been conducted to investigate the effect of CFRP strengthening technique on the structural behaviour of strengthened members under monotonic and cyclic loading. The results showed that the CFRP strengthening is effective to enhance the cyclic performance of CHS steel members by improving the moment capacity, moment degradation behaviour, secant stiffness,

energy dissipation capacity and ductility compared to bare steel CHS members. In addition, the moment capacity of CHSs has been improved under monotonic loading due to the CFRP strengthening as well. Moreover, the impact of adhesive types on the structural response of the strengthened specimens was also investigated. This information will be helpful in the strengthening of CHSs for their intended applications.

**KEYWORDS**

Circular Hollow Section (CHS) Steel members, Carbon fibre reinforced polymer (CFRP), Strengthening, Monotonic loading, Cyclic loading.

## 1. Introduction

Tubular hollow members become very popular in civil infrastructure and used broadly in the steel frame and truss industries for both architectural and structural purposes. This popularity can be ascribed to the advantages affiliated with tubular hollow members compared to the other open members, including in compression, bending and torsion in all directions, higher corrosion resistance capability as no sharp edges, fire protection ability by pouring water within the tube and aesthetics [1]. Earthquake is very destructive natural disasters which have caused massive destruction of property and human casualties. Earthquakes have been the reason for 1.87 million deaths in the 20th century. During 1990-2010, an average of 2052 fatalities per earthquake has been occurred [2]. Steel frames and trusses have been extensively constructed in seismic regions and CHSs are one of the major element of those structures. In halls and buildings, CHSs are mostly used for columns, roofs space frames or lattice girders. Nowadays, CHSs are also used in facades for structural and architectural reasons [1]. But nowadays the fracture failures of the structural elements due to cyclic loads in the structure during earthquake excitations have become a major concerned [3,4]. Earthquake not only causes extensive destruction of onshore structures but also cause extensive destruction of offshore structures as

well. Jacket type steel structures are one of the most common offshore structures and are constructed by welding of tubular members in the form of a space frame. The purpose of those structures is to support platforms for gas and oil production. Offshore structures are subjected to cyclic loads not only from the earthquake but also from currents, waves and wind [4]. Moreover, a huge number of steel structures can be found structurally deficient due to service loads increment, errors in design, effect of severe environments or loss of material properties. To address this phenomenon strengthening or rehabilitation of tubular structural sections to sustain large cyclic loads in seismic regions has received much attention by researcher nowadays. However, the study of the behaviour of tubular structural sections is more limited, especially under cyclic loading.

Traditionally, welding of additional steel plates is the most common method to rehabilitate and repair the steel structure. As a result of this method with the addition of extra weight to the structure, the stress distribution can be affected due to the heat involved during the welding process also; which can be critical for structures such as steel bridges that are exposed to fatigue loads. Moreover, welding of steel plates would be susceptible to corrosion damage. For this method, heavy machinery and the use of scaffolding are required as well as service interruptions over long periods [4]. On the other hand, strengthening and rehabilitation methods by using carbon fiber reinforced polymer (CFRP) composites can overcome these drawbacks and have many other advantages over steel plates such as superior strength-weight ratio and high tensile strength [5], corrosion resistive [6], cost-effective as it requires less labor and preparation , easy applicability within limited access, higher flexibility and can form any required shape [7,8]. Past research has shown the effectiveness of the CFRP strengthening technique to increase the load carrying capacity [9], impact resistance capacity [10] and tip displacement reduction capacity of steel structures [11]. In addition, it has been found that there has been a delay in the local buckling [12,13] and improvement of the energy absorption

capacity of the steel members after being strengthening by CFRP reinforcement [14]. Another important advantage of CFRP strengthening technique is fatigue strengthening of steel joints [15–17]. With these in mind, a comprehensive experimental study has been performed with the aim to upgrade the structural performances of cantilever CHS members under monotonic and cyclic loading, which will be useful for rehabilitating members of high-risk structures in seismic regions by CFRP strengthening.

Although there are some studies reported on the bending behaviour of externally bonded CFRP reinforced steel hollow sections including CHS steel members [18–22], the cyclic responses of CFRP strengthened CHS steel members, as well as the bending behaviour of CFRP strengthened cantilever CHS steel members have not been studied yet. Hence, there is a lack of understanding about the effectiveness of CFRP wrapping of cantilever CHS steel members subjected to cyclic loading as well as subjected to monotonic loading. In the present experimental program, the performance of CFRP strengthened CHS steel members under cyclic loading as well as under monotonic loading are investigated by applying the loading at the tip of the structural member through a hydraulic actuator. Six specimens of CHS steel members of similar diameter, length, and wall thickness were prepared and CFRP was applied using two different types of adhesives (to evaluate the effects of this parameters) to strengthen the CHS members. Moment vs displacement graphs for the bare and strengthened CHS members under monotonic loading are first compared followed. This was followed by continued cycling effects to evaluate the behaviour of the bare and strengthened CHS members with respect to the moment capacity, moment degradation, secant stiffness, energy dissipation, ductility, the occurrence of local buckling and propagation of yielding along the length of the section.

## 2. Experimental Program

### 2.1 Materials

There are four materials that have been used in the proposed CFRP strengthening scheme, including steel tubes, normal modulus CFRP MBrace Fib 300/50 CFS sheet, Mbrace saturant of two-part epoxy resin and Araldite K630 of two-part epoxy resin. The CHS steel specimens were manufactured as Grade C250L conforming to AS/NZS 1163:2009 [23] and provided by OneSteel Limited (Brisbane, Australia). The modulus of elasticity, yield stress and ultimate strength of steel tube were found to be 190 GPa, 320 MPa and 367 MPa respectively according to AS1391:2007 [19]. CFRP composite sheet was used in this study to strengthen tubular members using epoxy adhesive. The CFRP material was a unidirectional MBrace Fib 300/50 CFS sheet and commonly known as a high-tensile-strength material. The experimental thickness of CFRP was measured in three different locations of the specimen using digital Vernier calipers. The average thickness of one layer CFRP laminate was 0.60 mm. Based on availability and the usage of adhesives in the Australian environment, two commonly available adhesives have been tested which are Mbrace saturant two-part epoxy-based resin and Araldite K630 two-part epoxy-based resin to find out the effect of adhesive types in the strengthening process. Among them, Araldite K630 has the high elastic modulus but less tensile strength. The measured material properties of CFRP and both types of adhesive were obtained from the previous studies done by one of the authors [25,26] according to ASTM D3039 [27]. The modulus of elasticity and tensile strength of CFRP, Mbrace saturant and Araldite K630 were 75 GPa and 987 MPa, 2.86 GPa and 46 MPa and 6.5 GPa and 33 MPa respectively.

### 2.2 Experimental Specimens and Strengthening Schemes

A total of six CHS specimens were prepared to test under monotonic and cyclic loading during this study. Two of them are bare beams which were kept as control specimens. The

strengthened beams are classified based on types of adhesive. There are three parts in the specimen label: in the first part, BB denotes bare beam members and SB denotes the CFRP strengthened steel beam members. In the second part, M represents the testing under monotonic loading and C represents the testing under cyclic loading. In the last part, 1 represents the first type of adhesive Mbrace saturant and 2 represents the second type of adhesive Araldite K630 respectively. The details of the specimens and the experimental matrix are given in Table 1.

Table 1: Details of Experimental Specimens

| Specimen identifier | Specimen types | Loading condition | Adhesive types |
|---|---|---|---|
| BB-M | Bare Beam | Monotonic | - |
| SB-M-1 | Strengthened Beam | Monotonic | Mbrace saturant |
| SB-M-2 | Strengthened Beam | Monotonic | Araldite K630 |
| BB-C | Bare Beam | Cyclic | - |
| SB-C-1 | Strengthened Beam | Cyclic | Mbrace saturant |
| SB-C-2 | Strengthened Beam | Cyclic | Araldite K630 |

All the CHS steel members with the outer diameter and wall thickness of 101.6 mm and 4 mm respectively were fabricated in lengths of 1,300 mm from 6,500 mm cold-formed steel pipes. Strengthened beams are wrapped with same 900 mm bond length of CFRP and with same CFRP fibre LHL orientation. LHL means that in the first layer CFRP fibres are in the longitudinal direction, in the second layer CFRP fibres are in hoop direction and in the third layer CFRP fibres are in the longitudinal direction again. The CFRP fibre orientation of LHL was chosen as it was shown better performance than others in a previous study [25]. Figure 1 demonstrates the schematic diagram of the strengthening scheme.

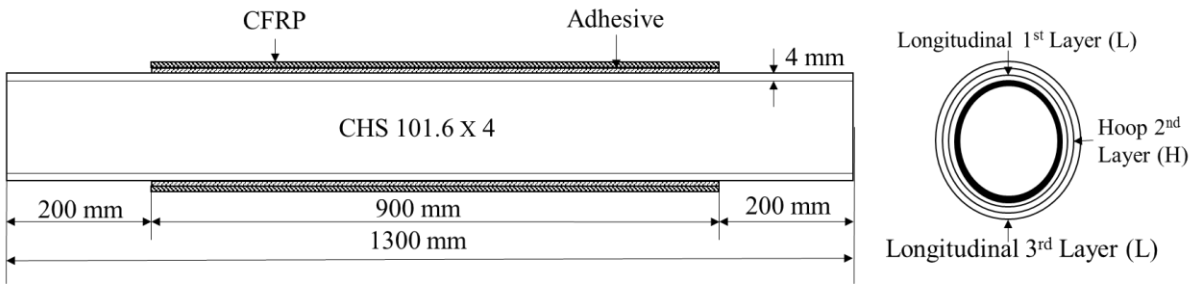


Figure 1: Schematic diagram of strengthening scheme

### 2.3 Specimen Preparation and Strengthening Process

Strengthening the CHS steel members by using externally bonded CFRP is the first stage in the specimen preparation. Initially, an appropriate surface preparation method is required to remove the impurities from the steel surface and ascertain the proper bonding between the steel outer surface and CFRP. Sandblasting or grit blasting methods are found as highly appropriate methods of surface preparation in previous studies [28]. The sandblasting method was hence chosen as surface preparation to prepare the steel outer surface of the CHS specimens. Sandblasting was performed by using the garnet abrasive system with an average grit size of 0.425 mm [25]. The outer surface of the sandblasted specimen was cleaned with acetone to remove the dust particles and week layers from the surface. In recent studies, the same method of surface preparation was used to ascertain the proper bonding between the steel surface and CFRP sheet [29,30]. Then both parts A and part B of epoxy adhesive were mixed with a ratio of 1:3 properly and applied during its pot life on the surface of primer treated CHS steel specimens. The dry CFRP was trimmed previously based on required sizes and fiber orientations of LHL. The CFRP sheet for 1$^{st}$ layer was applied on the adhesive treated steel surface. The applied CFRP sheets were rib rolled with an appropriate rib roller after immediately applying the CFRP along the fiber direction to get a uniform CFRP/epoxy composite surface and remove any entrapped bubbles. The rib rolling was continued until there was bleeding of adhesive through the CFRP fabrics to get a completely saturated CFRP fabric which will form a CFRP/epoxy composite plate after curing. The rest of two layers of CFRP

strengthening process were conducted by using the same procedure as the 1st layer. The whole strengthening process was performed on the wet surface of the previously applied layer to provide a single CFRP/epoxy composite laminate after the curing process. To get a good quality bonded and uniform thickness CFRP/epoxy laminate along the length of the wrapped specimen, the CFRP strengthened area was wrapped by masking tape after finishing the strengthening process as shown in Figure 2(b). The masking tape was removed after 24 hours of curing and all the strengthened CHS specimens were cured again under the ambient temperature for at least two weeks to ensure that full maturity has been achieved. The sample of bare and CFRP strengthened specimens are shown in Figure 3.

(a)

(b)

Figure 2: Details of specimen preparation: (a) sandblasted specimen; (b) Application of masking tape

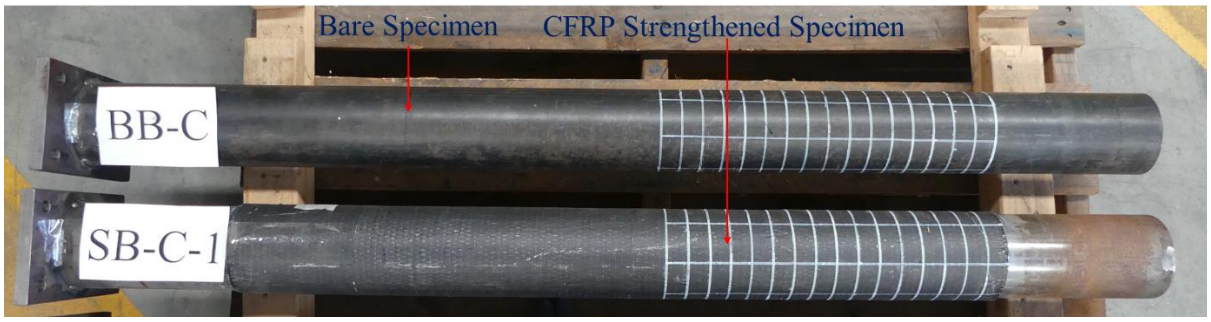


Figure 3: The sample of bare and CFRP strengthened specimens

### 2.4 Experimental Setup and Loading Protocol

The experimental setup to investigate the behaviour of the CHS members under monotonic and cyclic loading are shown in Figure 4 and Figure 5. The CHS beam member was cantilevered horizontally from the outside supporting frame in such a way so that the tip of the member will be under the testing frame. The input displacement was applied at the tip of the CHS member through two pinned hinges in order to prevent the application of any axial load and study the pure bending behaviour of the CHS members. The attached bearing endplate to the end of the member would prevent any local deformation during the application of loading. Although previous had research used four-point loading setup typically for investigating the bending behaviour of CHS under monotonic loading [25,28,31], cantilevered CHS members are used in this study to provide a better understanding of the hysteretic behaviour of CHS members and to form the plastic hinge at the support end of the members which would be expected in members during seismic events in a seismic moment resisting frame structure. To reuse the connection, the cantilever CHS members were fixed with supporting frame by sandwiching between two large steel half circles. The stiffeners were attached to confirm the occurrence of the inelastic deformation apart from the connection area. This experimental set up of the specimen will allow for the overall evaluation of the inelastic bending behaviour of CHS specimens subjected to monotonic and cyclic action.

A hydraulic actuator of 1000 kN loading capacity and capability to measure the applied load and displacement was used to apply the monotonic as well as the cyclic loading. The applied moment in each specimen was measured as the applied load multiplied by the span length of 1200 mm. Displacement measurements were obtained by using Laser Displacement Sensors (LDS) as shown in Figure 5. The CHS members were gridded with markers for further investigation of the bending behaviour within the plastic hinge region. To investigate the propagation of yielding along the length of the specimen with the continued cycle, strain gages were placed at the upper surface of the CHS specimens at 55 mm, 165 mm, 330 mm and 550 mm from the fixed connection.

An increasing end displacements loading protocol shown in Figure 6 was adopted to study the moment-rotation behaviour of CHS members under cyclic loading which simulated a far-field type earthquake as per ANSI/AISC 341-16 [3]. The reason for choosing that protocol is because the present seismic provisions specified that most of the joints deformation must occur in the beam member [3]. The loading protocol was applied with a quasi-static loading rate as a displacement control. The rotation of each specimen was measured by dividing the tip vertical displacement with the span length of 1200 mm. During the experiment, it was observed at the connection that all of the sections underwent a small amount of rigid rotation. As a result, none of the specimens could reach the full rotational level of 0.08 rad. To address this, LDS's were placed on the beam at the end of the fixed connection and at the connection to measure the specimen's rigid rotation. The actual rotation of the CHS members was calculated by subtracting the measured rigid rotation from the overall rotation where the overall rotation was measured by placing another LDS at the beam tip. Although all of the specimens failed to reach the full rotational level of 0.08 rad., they underwent a rotation of 0.071 rad.

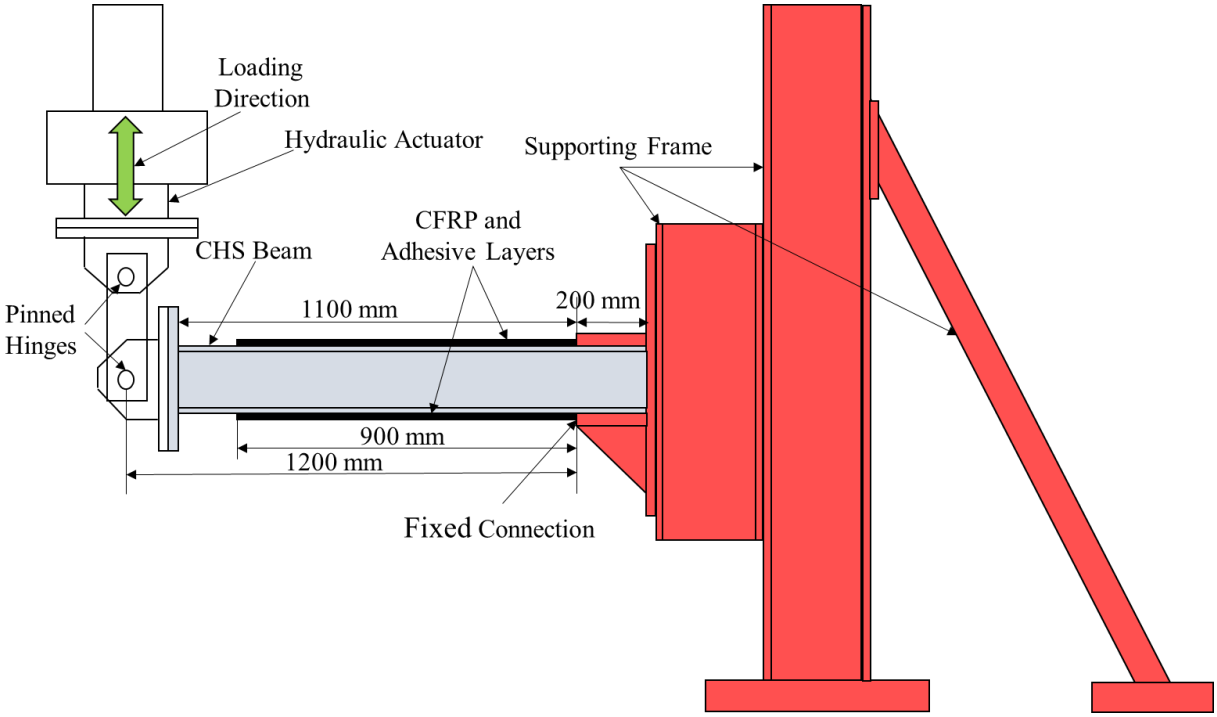


Figure 4: Schematic diagram of the experimental setup

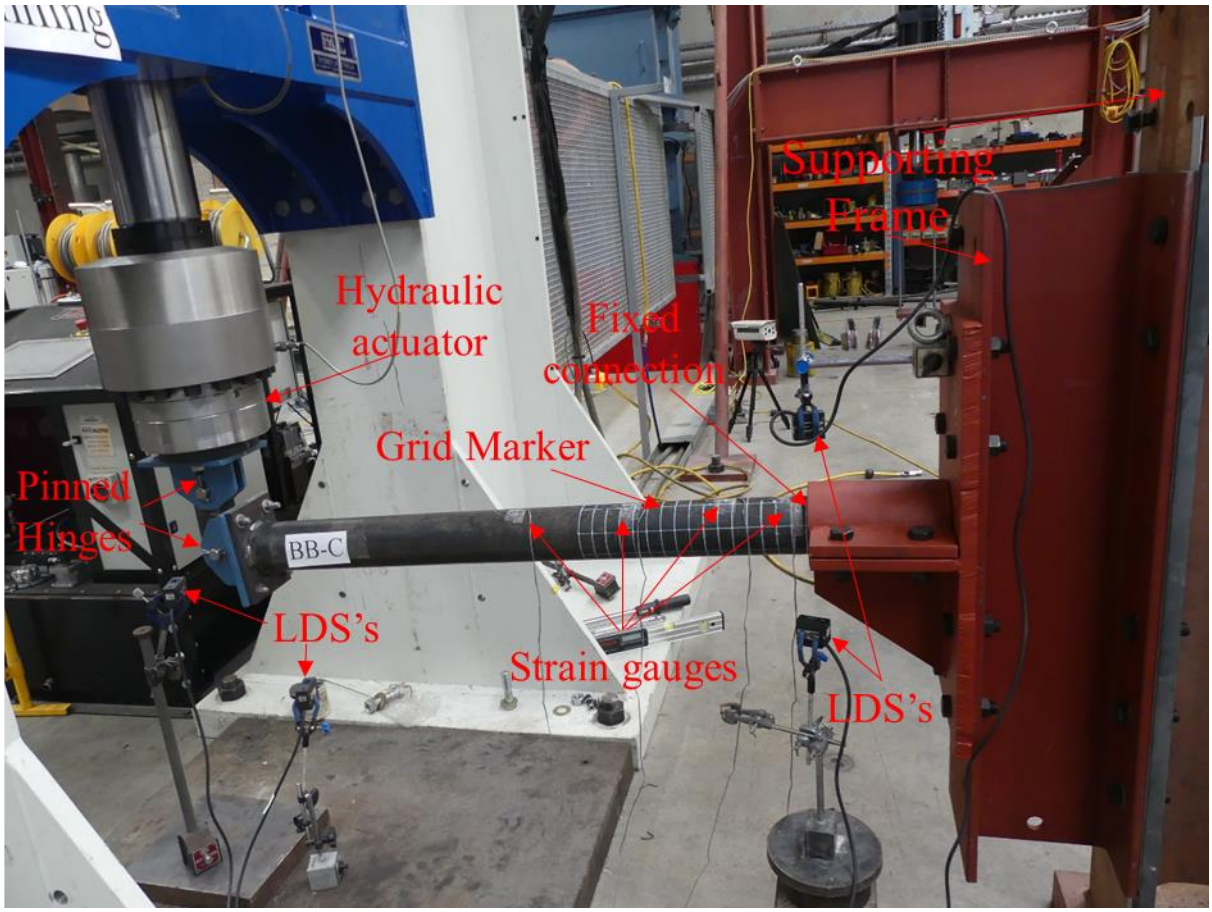


Figure 5: Photograph of the experimental setup

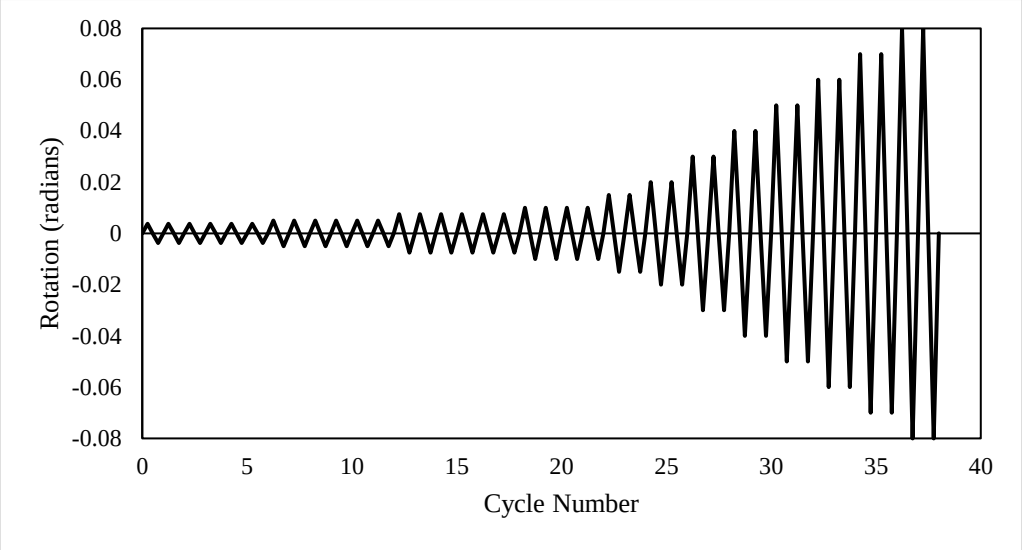


Figure 6: Experimental loading protocol (adopted from [3])

## 3. Experimental Results and Discussions

The CFRP strengthening technique helps to improve the moment capacity, hysteretic behaviour, stiffness, energy dissipation capacity and the ductility of CHS members by using the longitudinal fiber strength effectively and restraining the action of the hoop oriented fibers which have been confirmed by the results of the experimental study.

### 3.1 Experimental Monotonic Behaviour

Figure 7 shows the comparison of moment capacity versus displacement response between bare and CFRP strengthened CHS cantilever members under Monotonic loading. It is clear that the CFRP strengthening technique has a great influence in the improvement of moment capacity i.e. load carrying capacity of CHS member under monotonic loading. It can be seen that the moment capacity of CFRP strengthened CHS member has been increased by 33% compared to the unstrengthened bare member under monotonic loading due to using the LHL combination of the CFRP sheets. In addition, the present study showed a good agreement with the previous study on CFRP strengthened CHS member with the same LHL combination of the CFRP under pure four-point bending where the increment was 37% [25]. Hence, the

effectiveness of CFRP strengthening technique under the monotonic loading for CHS cantilever members has been confirmed by the present study.

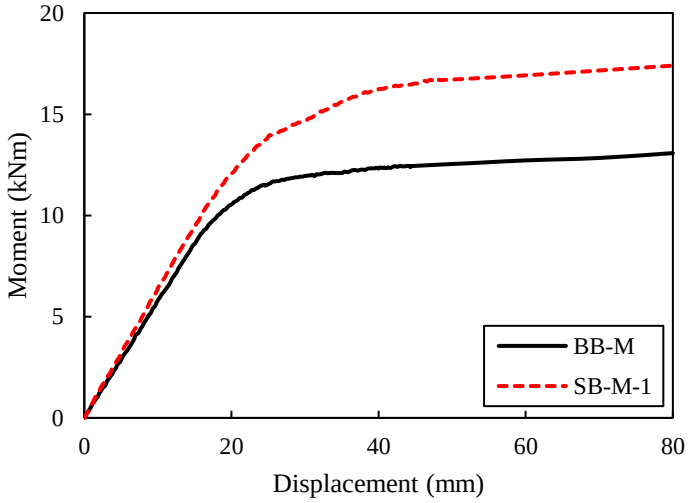


Figure 7: Moment capacity versus displacement response for bare and CFRP strengthened CHS members under Monotonic loading

### 3.2 Experimental Hysteretic Behaviour

The moment-rotation hysteresis was constructed to evaluate the cyclic hysteresis responses and the bending behaviour of the bare and CFRP strengthened CHS members. Figure 8(a) and Figure 8(b) show the moment-rotation hysteresis for the bare and CFRP strengthened CHS members respectively. Overall, it can be seen that both the bare and CFRP strengthened CHS members displayed the full hysteretic loops which ensured the appropriate inelastic behaviour. At the higher rotations levels (in the protocol), the moment capacity was decreasing during two successive cycles having the same level of rotation. This was also evident between one cycle and the next higher cycle of rotation. The effects of CFRP strengthening technique are observable as a noticeable improvement of moment capacity is observed for CFRP strengthened CHS specimen compared to the bare specimen under cyclic loading. The CFRP strengthened CHS specimen, SB-C-1, had the higher moment capacity of 17.10 kNm, while the unstrengthened (or bare) CHS specimen, BB-C, had the lower moment capacity of 12.90 kNm. Hence, after strengthening by CFRP the moment capacity has been improved by 32.5%.

In addition, the level of rotation, where the maximum moments were measured, is 0.05 rad. for the CFRP strengthened CHS specimen and 0.043 rad. for the unstrengthened (bare) CHS specimen.

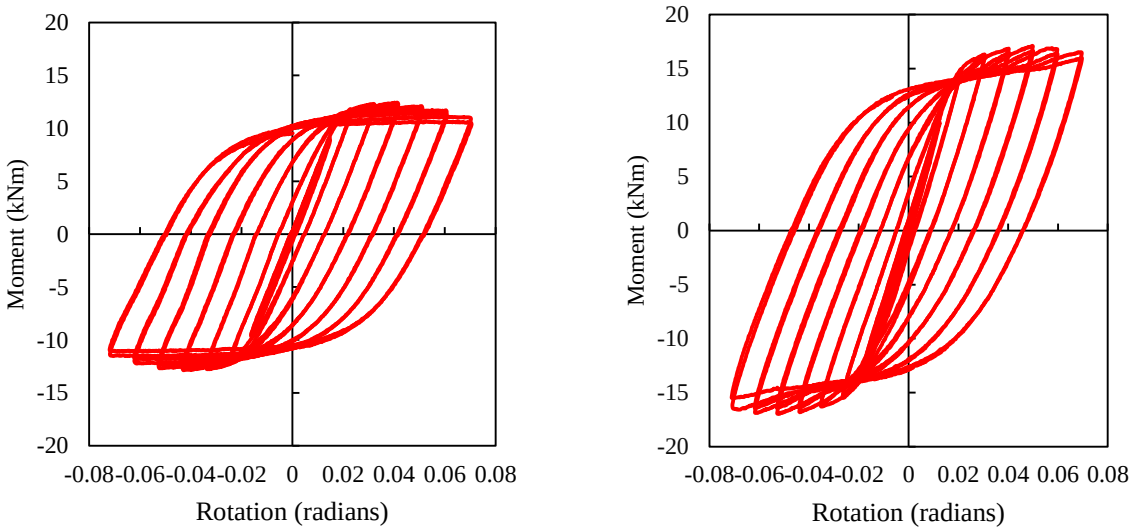


(a) (b)

Figure 8: Moment capacity versus rotation hysteresis responses of the (a) bare and (b) CFRP strengthened CHS members

### 3.3 Moment Capacity Degradation Behaviour

The moment versus rotation backbone curves of bare and CFRP strengthened CHS members have been generated by plotting moment against the maximum rotation of each cycle for further comparison of the hysteretic behaviour of bare and CFRP strengthened CHS members and shown in Figure 9. The backbone curves will also emphasis the previous outcomes from Figure 8. Both the bare and CFRP strengthened CHS members exhibited good symmetry in respect of positive and negative rotation which indicate a stable response in both directions.

At higher rotational levels, it is clear from the hysteretic behaviour [Figure 8] along with the backbone curves [Figure 9] of the bare and CFRP strengthened CHS members that the moment capacity is overall decreasing with consecutive cycling to reach next rotational level in both of the bare and CFRP strengthened CHS members. The onset of local buckling can be attributed

to the moment degradation which was more dominant for the unstrengthened CHS member. The CFRP strengthened CHS member showed more stable behaviour compared to the bare CHS member with less decrease of the moment capacity at the maximum rotational level even with consecutive cycles of larger rotational levels. It can be seen from the backbone curve of the CFRP strengthened CHS member that the maximum moment capacity was 17.1 kNm at the peak of the cycle of 0.05 rad. and the moment capacity was reduced to 16.52 kNm at the peak of the cycle of 0.07 rad. i.e. moment capacity has been dropped by only 3.4%. In contrast, the unstrengthened CHS member showed a higher drop of the moment capacity at the maximum rotational level from the maximum moment capacity. The maximum moment capacity of the unstrengthened bare CHS member was 12.90 kNm at 0.043 rad. and dropped by 11% to 11.50 kNm at 0.072 rad.

In addition, after the initiation of yielding, the moment capacity is also dropping in the successive cycling of the same rotation level along with consecutive cycling to reach next rotational level in the both of the bare and CFRP strengthened CHS members. Compared to bare CHS member, the CFRP strengthened CHS member showed a less percentage of reduction of moment capacity between the two successive cycles (across the same rotational range). This percentage reduction in the moment capacity due to cycling remained less than 4% throughout the full rotation for the CFRP strengthened CHS specimen, while in the bare CHS specimen it remained less than 6%.

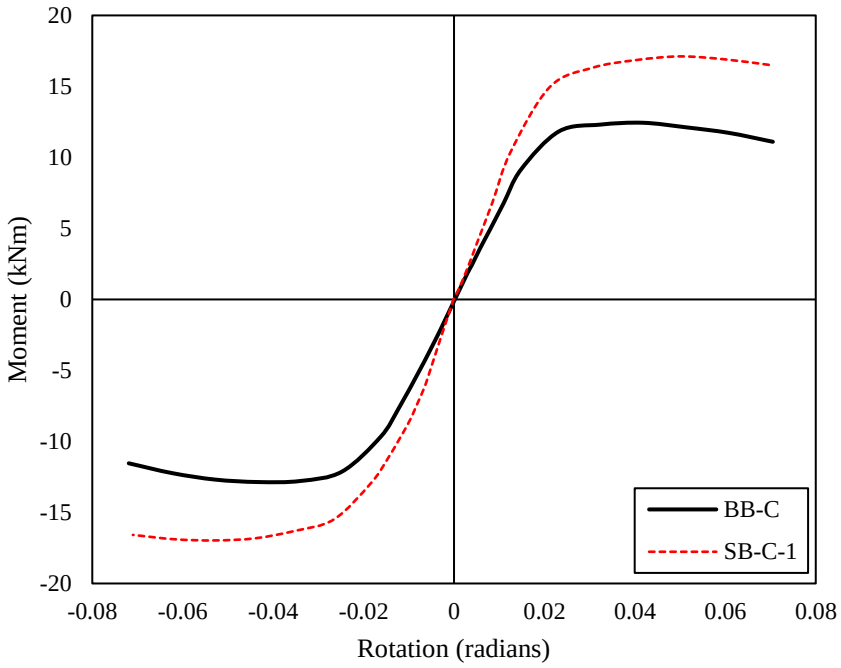


Figure 9: Moment versus rotation backbone curve for bare and CFRP-strengthened specimens

### 3.4 Secant Stiffness

The CFRP strengthening technique has a great influence on the changing of the secant stiffness with increasing the rotational level of the cycles. The secant stiffness of a particular cycle was measured by dividing the load at maximum displacement of that particular cycle with the maximum displacement of that particular cycle. A comparison of the secant stiffness between bare and the CFRP strengthened CHS specimens is shown in Figure 10. Overall, it is clear that the secant stiffness of both members was decreasing with increasing the rotational level of the cycles. The maximum secant stiffness of The CFRP strengthened CHS member is 536 kN⁄m at 0.009 rad., which is 25% higher than the secant stiffness of 429kN/m at 0.01 of the bare CHS member. In addition, although the bare and the CFRP strengthened CHS specimens were showing an almost similar trend of secant stiffness degradation, the CFRP strengthened CHS specimen underwent lower degradation of secant stiffness compared to the bare CHS specimen. The secant stiffness of the CFRP strengthened and bare CHS specimens dropped by 69.2% at the maximum rotation of 0.07 rad. and by 74.6% at the maximum rotation of 0.071 rad.

respectively from their maximum values. Moreover, at the end of testing i.e. at the maximum rotational cycle, the secant stiffness of the CFRP strengthened CHS specimen is 51.4% higher compared to the secant stiffness of the bare CHS specimen.

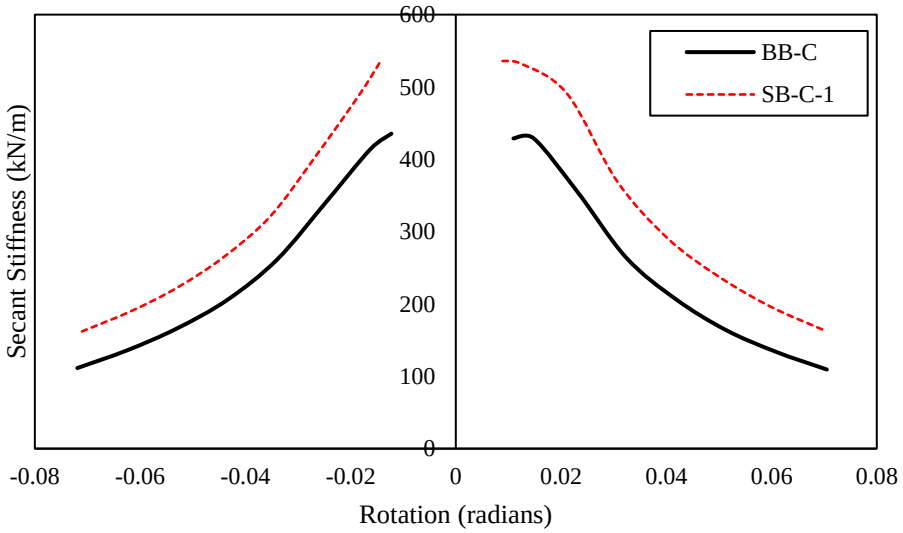


Figure 10: Secant stiffness versus rotation curve for bare and CFRP-strengthened specimens

### 3.5 Energy Dissipation Capacity

One of the main means of dissipating the input seismic energy is through inelastic deformation of specific elements. Typically frames dissipate energy through inelastic deformation of the beams, panel zones, and column bases. It is therefore important to consider the energy dissipation capacity of the members, both strengthened and bare, to gain a sense of the member's ability to dissipate the input energy during an earthquake. The energy dissipation capacity is calculated for each rotation level by measuring the hysteretic energy dissipation of a single cycle in a rotational level [32] and can be defined by the equation:

$$E = S_{ABCDA}$$

Where $S_{ABCDA}$ is the enclosed area under hysteresis loops ABCD (shaded area of Figure 11).

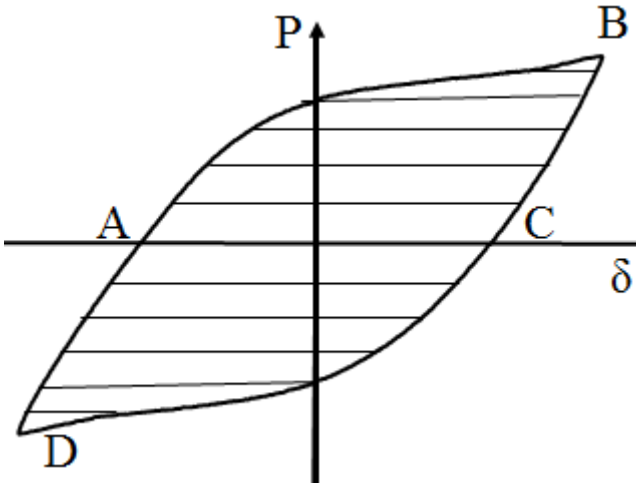


Figure 11: Calculation of energy dissipation capacity

Figure 12 plots the energy dissipation for the bare and the CFRP strengthened CHS members at the first cycle of every rotational level. In general, both the bare and the CFRP strengthened CHS members have been able to complete the full hysteretic curves which indicate that they have the capacity for energy dissipation. Up to a rotation of 0.0125 rad., the energy dissipated remained very small for both of the bare and the CFRP strengthened CHS members, since the connections essentially behaved elastically. At low rotational levels i.e. up to 0.0125 rad., the energy dissipated by the CFRP strengthened CHS specimen was slightly lower than that by the bare CHS specimen, although these are quite small. This was mainly due to the initial high stiffness due to CFRP wrapping. Up to the 0.043 rad. rotation cycle i.e. before reaching the ultimate moment capacity of the bare specimen, the energy dissipated by the CFRP strengthened CHS specimen was slightly higher than that by the bare CHS specimen. This shows that the initial high stiffness due to CFRP wrapping has still an effect on the energy dissipation capacity. After the 0.043 rad. rotation cycle i.e. after reaching the ultimate moment of the bare specimen, it is clear that the increment of energy dissipation capacity of the CFRP strengthened CHS specimen is much higher than the bare specimen. At the end of the experiment i.e. at the maximum rotation level, the energy dissipation capacity of the CFRP strengthened CHS specimen is 2.45 kNm, while it is 2.08 kNm for the bare CHS specimen. It is hence evident that the energy dissipation capacity has improved by 18% due to CFRP

wrapping and shows that the seismic performance of the CFRP wrapped member can be expected to be superior to that of the specimen without any strengthening.

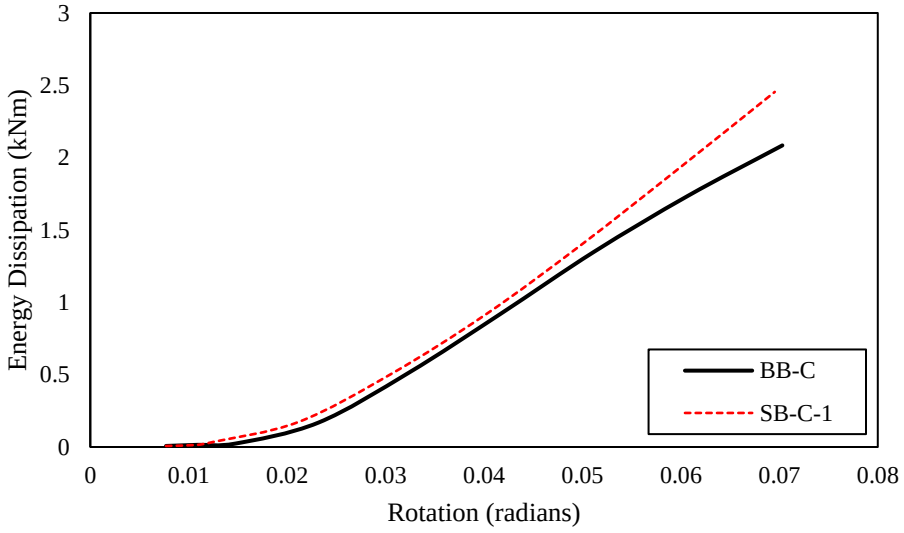


Figure 12: Energy dissipation versus rotation curve for bare and CFRP-strengthened specimens

### 3.6 Ductility

Ductility is an important parameter for earthquake resistant structures. The CHS members must have the ability to generate stable plastic hinges with adequate moment capacity and ductility under continued cycling effects in order to be considered for the seismic applications. The displacement ductility index μ is computed by dividing the ultimate lateral displacement, $\delta_u$ by the yield lateral displacement, $\delta_y$ to evaluate the ductility of a member. $\delta_u$ and $\delta_y$ can't be obtained directly from the present hysteretic curves as there was no apparent yield point observed in the present hysteretic curves. There are generally two approaches, such as the general yield moment method and the equivalent energy method, to determine $\delta_{y,}$ when there is no apparent yield point in the hysteretic curves, [33]. Figure 13(a) displays the general yield moment method. The tangent line passed through Origin O and the tangent line on the peak point M of the curve were intersected at Point A. Then the point B is the intersected point of the curve and the vertical line passing through the Point A. The line through the point O and

point B is intersected with tangent line on the peak point M of the curve at point C. Finally, the approximate yield point Y is the intersected point of the curve and the vertical line passing through the Point C. Figure 13(b) shows the equivalent energy method, where the approximate yield point Y is determined when the shaded areas of (1) and (2) are made equal. As there are so many approaches for the equivalent energy method, the general yield moment method has been chosen for the present study to determine $\delta_y$. The ultimate lateral displacement $\delta_u$ was the lateral displacement corresponding to the 90% of the ultimate loads $P_u$ [34].

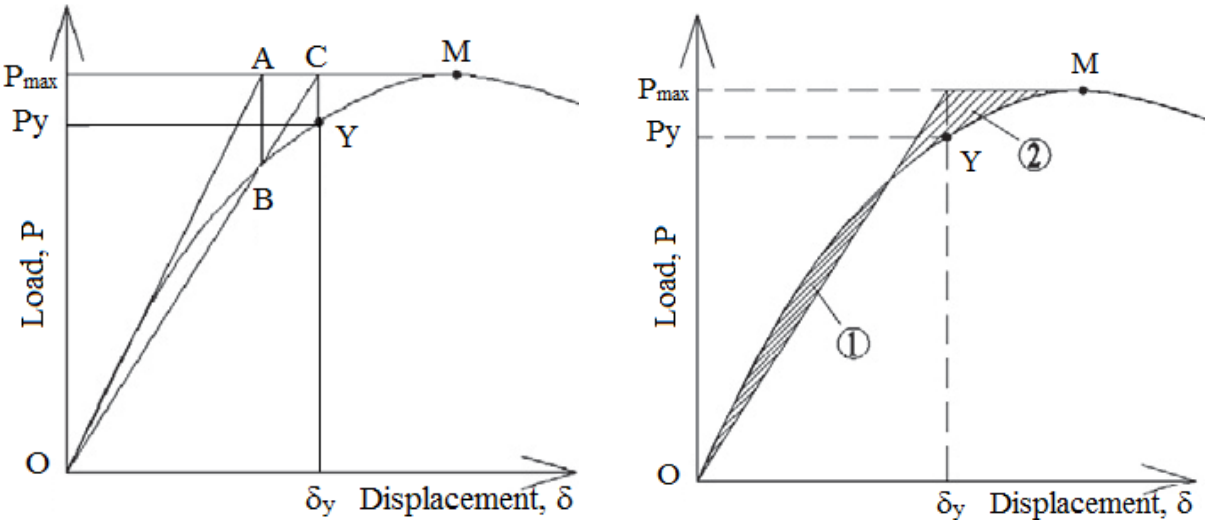


Figure 13: (a) The general yield moment method and (b) The equivalent energy method to determine the approximate yield point

Figure 14 depicts the ductility index evaluated by general yield moment method for the bare and CFRP strengthened CHS specimens. The influence of CFRP strengthening technique to enhance the ductility of the CHS beam is evident from the Figure 14. As a result of CFRP strengthening technique, the ductility of the CHS member has been improved by 13% in the positive rotation and 10.5% in the negative rotation.

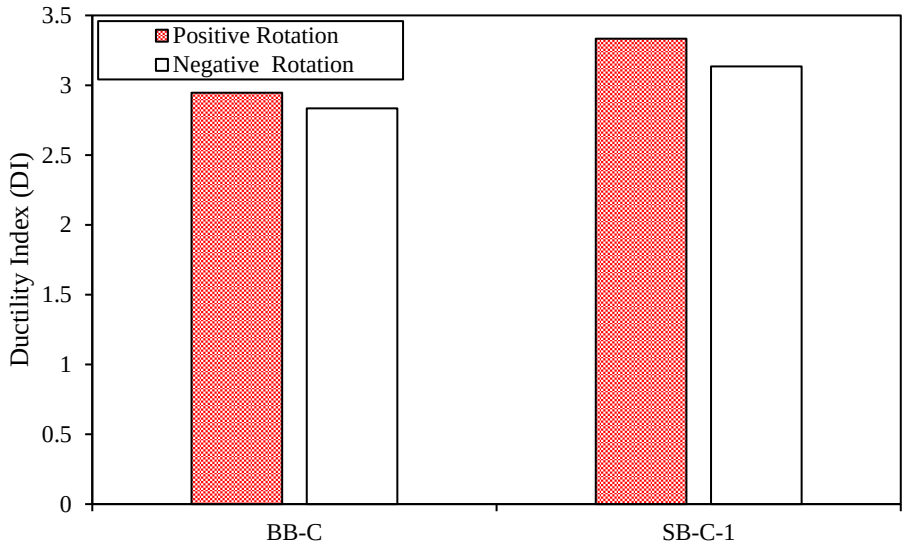


Figure 14: Ductility Index for bare and CFRP-strengthened specimens

### 3.7 Effect of Adhesive Type

Mbrace saturant and Araldite K630 are two usually available adhesives and used to investigate the effect of adhesive types on the CFRP strengthened CHS members under monotonic and cyclic loading. Figure 15-Figure 20 shows the comparison of the different structural properties between strengthened CHS specimens with the Mbrace saturant and Araldite K630 adhesives. It can be seen that the strengthened CHS members with the Mbrace saturant and Araldite K630 are shown very close performance. Although tensile strength of the Mbrace saturant is higher than the Araldite K630, its stiffness is lower than the Araldite K630. Thus, CFRP properties are the governing factors instead of the adhesive properties on the CFRP strengthening technique. The strengthened CHS members with the Araldite K630 shows slightly better behaviour in terms of moment capacity, secant stiffness and energy dissipation as Araldite K630 is stiffer compared to Mbrace saturant. On the other hand, the strengthened CHS members with the Mbrace saturant is performed slightly better in terms of the moment degradation behaviour and ductility index as the tensile strength of the Mbrace saturant is higher than the tensile strength of the Araldite K630.

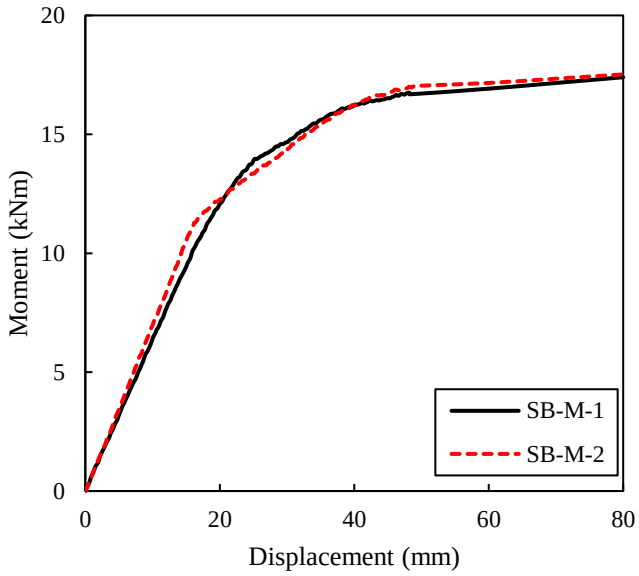


Figure 15: Moment capacity versus displacement relationship of strengthened CHS members with different types of adhesive under Monotonic loading

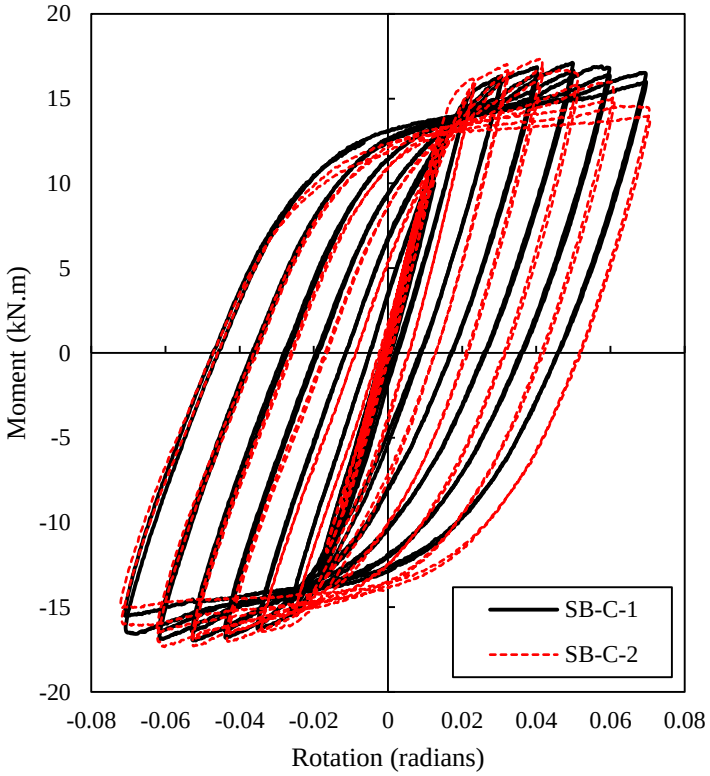


Figure 16: Moment versus rotation hysteresis curve of strengthened CHS members with different types of adhesive

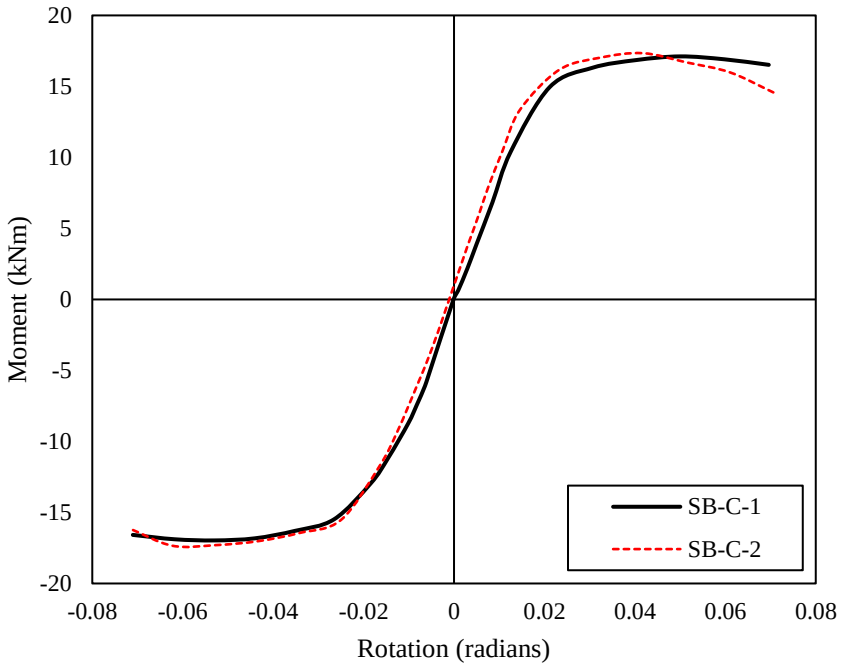


Figure 17: Moment versus rotation backbone curve of strengthened CHS members with different types of adhesive

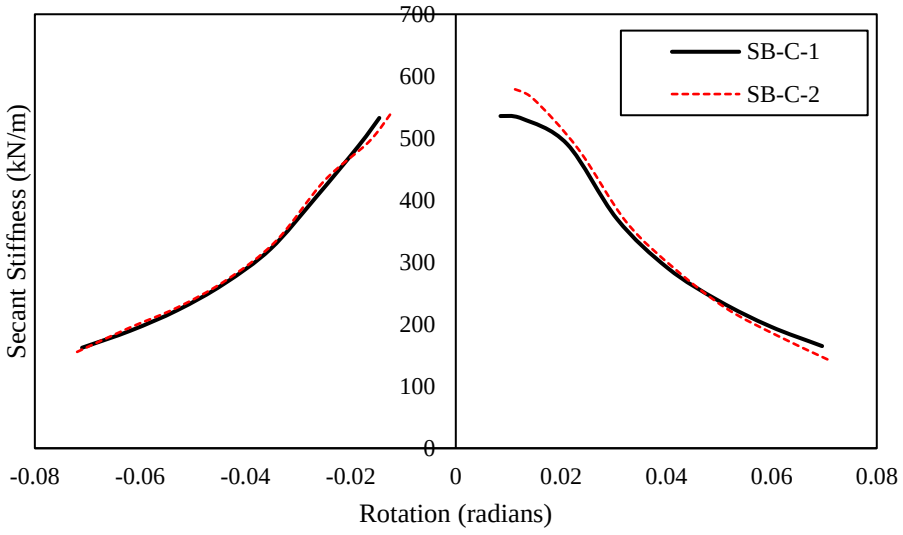


Figure 18: Secant stiffness versus rotation relationships of strengthened CHS members with different types of adhesive

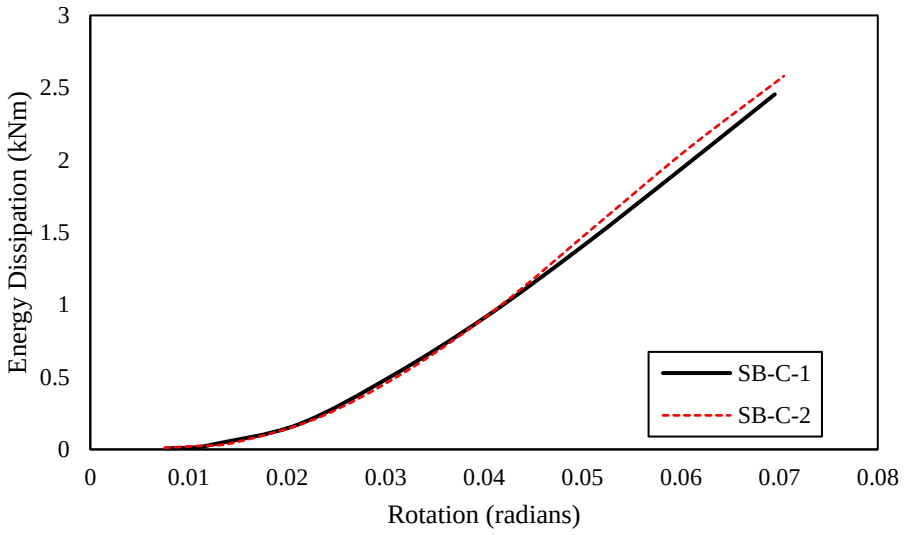


Figure 19: Energy dissipation versus rotation relationships of strengthened CHS members with different types of adhesive

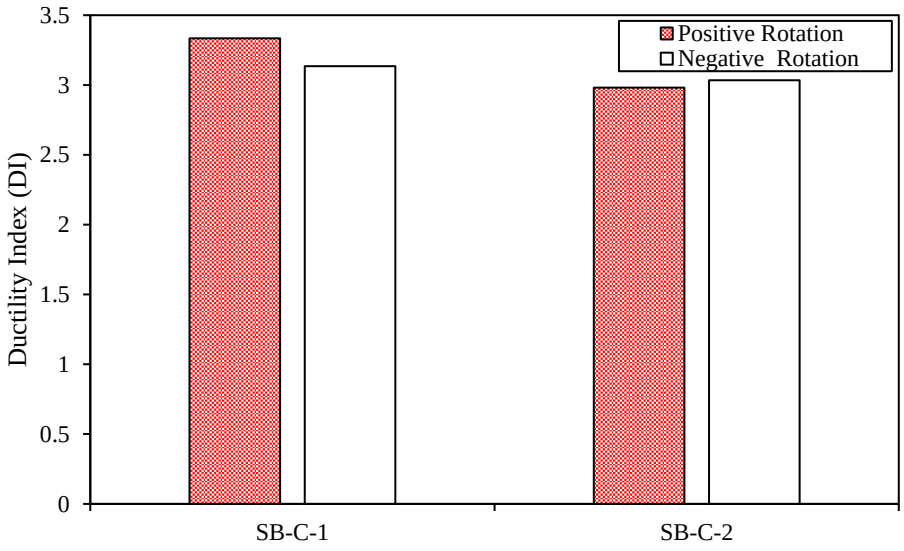


Figure 20: Comparison of ductility Index of strengthened CHS members with different types of adhesive

### 3.8 Plastic Hinge Development

The strain distribution characterization along the length of the members allowed for investigating the yield propagation along the length of the members. So strain gauges were placed in the top surface of the members at the distances of 55 mm, 165 mm, 330 mm and 550 mm from the rigid connection to measure the strain along the length of the members. The yield strain of the bare CHS member is 0.00154 determined based on its yield stress. A comparison

study of strains has been conducted at the member overall rotational levels of 0.01 rad., 0.04 rad., 0.06 rad. and 0.08 rad., where the member rotational levels of 0.01 rad., 0.04 rad., 0.06 rad. and 0.08 rad. represent small, medium, high and very high rotation levels respectively. Figure 21, Figure 22 and Figure 23 display the comparison study for the bare beam, strengthened beam SB-C-1 and strengthened beam SB-C-2 respectively.

At the rotation level of 0.01 rad., the bare member remained elastic under both compression and tension. At the rotation level of 0.04 rad., yielding in the bare member has been propagated to at least 330 mm from the fixed end under both compression and tension. At the rotation level of 0.06 rad. and 0.08 rad., the strains at 165 mm, 330 mm and 550 mm from the fixed end of the bare member have been reduced compared to strains measured in the preceding rotational levels. Therefore the bare specimen underwent the onset of local buckling in both compression and tension at less than 165 mm from the fixed end where most of the successive inelastic deformation has occurred. In contrast, the measured strains of both of the CFRP strengthened beams has been increased up to the rotational level of 0.06 rad. in both compression and tension. At the rotational level of 0.08 rad., the strains at 165 mm, 330 mm and 550 mm from the fixed end of both of the CFRP strengthened members have been reduced compared to strains measured in the preceding rotational levels. Hence after being CFRP strengthened the rotational capacity of the member has been improved and the local buckling has been delaying from the overall rotational level of 0.06 rad. to 0.08 rad..

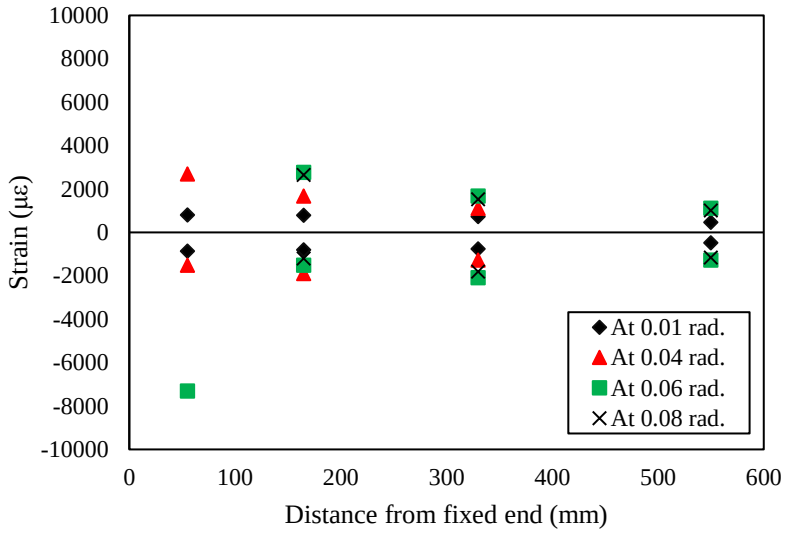


Figure 21: Strain along the length of Bare Beam

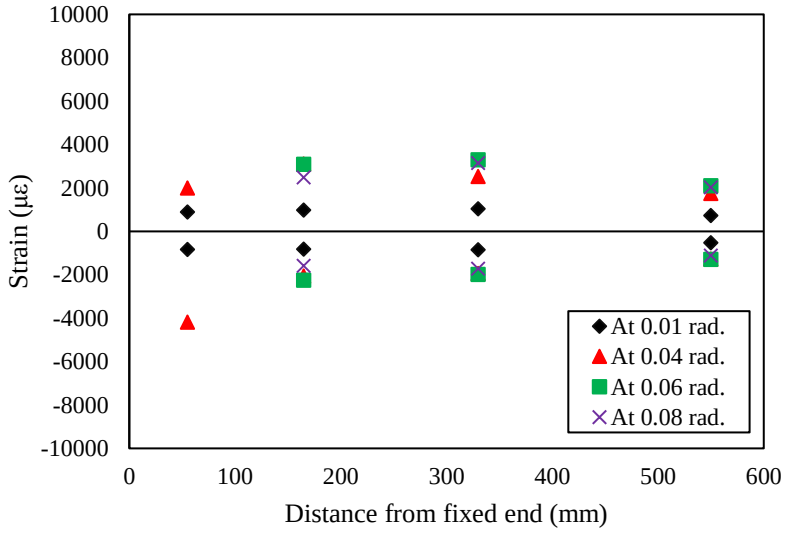


Figure 22: Strain along the length of Strengthened beam SB-C-1

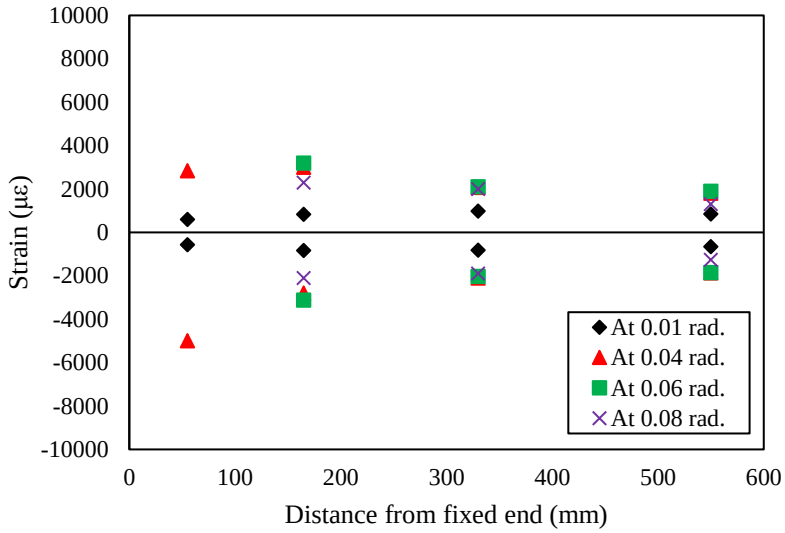


Figure 23: Strain along the length of Strengthened beam SB-C-2

## 4. Conclusions

The behaviour of CFRP unstrengthened and bare CHS steel member under both monotonic and cyclic loading has been investigated in this paper through an experimental study. From the experimental results, it can be concluded that the CFRP strengthening technique is very effective for improving the behaviour of CHS steel member under both monotonic and cyclic loading. The major observations and outcomes based on the results of this study are summarized as follows:

1. The moment-deformation relationship of both bare and CFRP strengthened CHS steel members obtained under monotonic loading are very similar to their hysteretic relationship envelops under cyclic loading which was expected as the utilization of the material hardening criteria was very small and consequently insufficient to simulate bauschinger effect. Therefore cyclic loading has very little effect on both bare and CFRP strengthened CHS steel members' moment capacity and this signifies that the monotonic behaviour would provide sufficient envelope for hysteretic behaviour of bare and CFRP strengthened CHS steel member.

2. The beneficial effects of the CFRP strengthening technique are evident as there is a significant improvement of moment-deformation relationship and hysteresis behaviour for CFRP strengthened CHS specimen compared to the bare specimens under monotonic and cyclic loading. The CFRP strengthened CHS steel member with three layers of CFRP of LHL configuration and Mbrace saturant adhesive showed 33% and 32.5% higher moment capacity than the unstrengthened bare CHS steel member under monotonic and cyclic loading respectively.
3. The more stable behaviour was shown by the CFRP strengthened CHS steel members with very small degradation of moment capacity compared to the bare (or unstrengthened) CHS steel member.
4. The stiffness of the CFRP has a noticeable effect on the strengthening of CHS steel member. This is the reason why CFRP strengthened CHS steel members show a higher maximum secant stiffness with less degradation of secant stiffness compared to bare CHS steel member.
5. The CFRP strengthened CHS steel members shows a higher ability to dissipate the input energy and larger ductility index during cyclic loading than the bare CHS steel member which proved that the cyclic performance of the CFRP strengthened member is expected to be superior to that of the member without any strengthening.
6. The properties of adhesive do not have much effect on the overall structural performance of CFRP strengthened CHS steel members as the stiffness of the CFRP is the dominant factor in the strengthening of CHS steel member.
7. The CFRP strengthening technique has improved the rotational capacity of the CHS steel member by delaying the local buckling from the overall rotational level of 0.06 rad. to 0.08 rad..

**Acknowledgment**

The authors wish to thank the technical staff, Mr. Frank De Bruyne, Mr. Glenn Atlee and Mr. Barry Hume for their assistance in conducting the experimental study reported in this research at the Banyo Pilot Plant Precinct of Queensland University of Technology (QUT). The authors also wish to thank Dr. Md Humayun Kabir and Dr. Sanam Aghdamy for their assistance in specimen preparation and experimental work respectively. The authors also wish to thank the School of Civil Engineering & Built Environment at the Queensland University of Technology (QUT), Australia for the financial support for the experimental work reported in this study.

**Reference**

[1] Wardenier J, Packer JA, Zhao XL, Van der Vegte GJ. Hollow sections in structural applications. Bouwen met Staal Rotterdam,, The Netherlands; 2002.

[2] Guha-Sapir D, Below R, Hoyois P. EM-DAT: International disaster database. Cathol Univ Louvain Brussels, Belgium 2015.

[3] ANSI/AISC 341-16. Seismic Provisions for Structural Steel Buildings. Am Inst Steel Constr 2016:402. doi:111.

[4] Seica M V., Packer JA. FRP materials for the rehabilitation of tubular steel structures, for underwater applications. Compos Struct 2007;80:440–50. doi:10.1016/j.compstruct.2006.05.029.

[5] Batuwitage C, Fawzia S, Thambiratnam DP, Tafsirojjaman T, Al-Mahaidi R, Elchalakani M. CFRP-wrapped hollow steel tubes under axial impact loading. Tubul. Struct. XVI Proc. 16th Int. Symp. Tubul. Struct. (ISTS 2017, 4-6 December 2017, Melbourne, Aust., CRC Press; 2017, p. 401.

[6] Hollaway LC, Teng J-G. Strengthening and rehabilitation of civil infrastructures using fibre-reinforced polymer (FRP) composites. Elsevier; 2008.

[7] Teng JG, Chen JF, Smith ST, Lam L. Behaviour and strength of FRP-strengthened RC structures: a state-of-the-art review. Proc Inst Civ Eng - Struct Build 2003;156:51–62. doi:10.1680/stbu.2003.156.1.51.

[8] Zhao XL, Zhang L. State-of-the-art review on FRP strengthened steel structures. Eng Struct 2007;29:1808–23. doi:10.1016/j.engstruct.2006.10.006.

[9] Kabir MH, Fawzia S, Chan THT, Gamage JCPH. Comparative durability study of CFRP strengthened tubular steel members under cold weather. Mater Struct 2016;49:1761–74. doi:10.1617/s11527-015-0610-x.

[10] Alam MI, Fawzia S, Tafsirojjaman T, Zhao XL. FE modeling of FRP strengthened CHS members subjected to lateral impact. Tubul. Struct. XVI Proc. 16th Int. Symp. Tubul. Struct. (ISTS 2017, 4-6 December 2017, Melbourne, Aust., CRC Press; 2017, p. 409.

[11] Tafsirojjaman T, Fawzia S, Thambiratnam D, Zhao XL. Seismic strengthening of rigid steel frame with CFRP. Arch Civ Mech Eng 2019;19:334–47. doi:10.1016/j.acme.2018.08.007.

[12] Harries KA, Peck AJ, Abraham EJ. Enhancing stability of structural steel sections using FRP. Thin-Walled Struct 2009;47:1092–101. doi:10.1016/j.tws.2008.10.007.

[13] Fernando ND. Bond behaviour and debonding failures in CFRP-strengthened steel members. The Hong Kong Polytechnic University, 2010.

[14] Alam MI, Fawzia S. Numerical studies on CFRP strengthened steel columns under transverse impact. Compos Struct 2015;120:428–41. doi:10.1016/j.compstruct.2014.10.022.

[15] Nakamura H, Jiang W, Suzuki H, Maeda K ichi, Irube T. Experimental study on repair of fatigue cracks at welded web gusset joint using CFRP strips. Thin-Walled Struct 2009;47:1059–68. doi:10.1016/j.tws.2008.10.016.

[16] CHEN T, YU Q-Q, GU X-L, ZHAO X-L. Study on Fatigue Behaviour of Strengthened Non-Load-Carrying Cruciform Welded Joints Using Carbon Fiber Sheets. Int J Struct Stab Dyn 2012;12:179–94. doi:10.1142/S0219455412004586.

[17] Xiao Z-G, Zhao X-L. CFRP repaired welded thin-walled cross-beam connections subject to in-plane fatigue loading. Int J Struct Stab Dyn 2012;12:195–211.

[18] Haedir J, Bambach MR, Zhao XL, Grzebieta RH. Strength of circular hollow sections (CHS) tubular beams externally reinforced by carbon FRP sheets in pure bending. Thin-Walled Struct 2009;47:1136–47. doi:10.1016/j.tws.2008.10.017.

[19] Photiou N, Hollaway LC, Chryssanthopoulos MK. Strengthening Of An Artificially Degraded Steel Beam Utilising A Carbon/Glass Composite System. Adv Polym Compos Struct Appl Constr ACIC 2004 2004;20:274–83. doi:10.1016/B978-1-85573-736-5.50030-3.

[20] Haedir J, Zhao XL, Grzebieta RH, Bambach MR. Non-linear analysis to predict the momentcurvature response of CFRP-strengthened steel CHS tubular beams. Thin-Walled Struct 2011;49:997–1006. doi:10.1016/j.tws.2011.03.004.

[21] Haedir J, Zhao XL. Design of CFRP-strengthened steel CHS tubular beams. J Constr Steel Res 2012;72:203–18. doi:10.1016/j.jcsr.2011.12.004.

[22] Haedir J, Zhao XL, Bambach MR, Grzebieta RH. Analysis of CFRP externally-reinforced steel CHS tubular beams. Compos Struct 2010;92:2992–3001. doi:10.1016/j.compstruct.2010.05.012.

[23] Standard A. Cold-formed structural steel hollow sections. AS 11632009, Aust 2009.

[24] Standard A. Metallic materials—tensile testing at ambient temperature. AS 1391-2007, Aust 2007.

[25] Kabir MH, Fawzia S, Chan THT, Gamage JCPH, Bai JB. Experimental and numerical investigation of the behaviour of CFRP strengthened CHS beams subjected to bending. Eng Struct 2016;113:160–73. doi:10.1016/j.engstruct.2016.01.047.

[26] Alam I, Fawzia S, Zhao X, Asce F, Remennikov AM. Experimental Study on FRP-Strengthened Steel Tubular Members under Lateral Impact 2013;21. doi:10.1061/(ASCE)CC.1943-5614.0000801.

[27] Standard A. Standard test method for tensile properties of polymer matrix composite materials. ASTM D3039/D M 2008;3039:2008.

[28] Kabir MH, Fawzia S, Chan THT, Badawi M. Durability of CFRP strengthened steel circular hollow section member exposed to sea water. Constr Build Mater 2016;118:216–25. doi:10.1016/j.conbuildmat.2016.04.087.

[29] Tafsirojjaman, Fawzia S, Thambiratnam D. Enhancement Of Seismic Performance Of Steel Frame Through CFRP Strengthening. Procedia Manuf 2018;Accepted.

[30] Batuwitage C, Fawzia S, Thambiratnam D, Al-Mahaidi R. Durability of CFRP strengthened steel plate double-strap joints in accelerated corrosion environments. Compos Struct 2017;160:1287–98. doi:10.1016/j.compstruct.2016.10.101.

[31] Kabir MH, Fawzia S, Chan THT, Gamage JCPH. Durability performance of carbon fibre-reinforced polymer strengthened circular hollow steel members under cold weather. Aust J Struct Eng 2014;15:377–92. doi:10.7158/S13-042.2014.15.4.

[32] Jacobsen LS. Steady forced vibration as influenced by damping. Trans ASME-APM

1930;52:169–81.

[33] Li ZX. Theory and technique of engineering structure experiments 2004.

[34] Paulay T. Equilibrium criteria for reinforced concrete beam-column joints. Struct J 1989;86:635–43.